SEASONAL SNOW COVER EXTENT FROM MICROWAVE REMOTE SENSING DATA: COMPARISON WITH EXISTING GROUND AND SATELLITE BASED MEASUREMENTS

Arnaud Mialon[1,2], Michel Fily[1] and Alain Royer[2]

1. Laboratoire de Glaciologie et Géophysique de l'Environnement, Université Joseph Fourier / CNRS, Grenoble, France; {mialon / fily}(at)lgge.obs.ujf-grenoble.fr
2. Université de Sherbrooke, Centre d'Applications et de Recherches en Télédétection, Sherbrooke, Canada (Québec); alain.royer(at)usherbrooke.ca

ABSTRACT

A significant response of global warming is expected to occur over the high latitudes. Due to the presence of permafrost and snow cover these regions are very sensitive to an increase in air temperature. Our objective is to derive a daily Snow Cover Extent variation from satellite microwave sensors over Canada-Alaska and Northern Eurasia (latitudes >50°N), as *in situ* measurements do not allow a study over northern high latitudes. Passive microwave data from SSMI (Special Sensor Microwave Imager) sensors are adequate for this study as they can measure the energy emitted by the earth surface, independent of solar illumination and cloud cover. Here, we are presenting a simple method based on vertically polarized brightness temperatures at 19 and 37 GHz and the determination of an adaptative threshold.

The study of the 1988-2002 mean seasonal snow extent shows a maximum snow cover for mid-February of $(9.69+/-0.06)\cdot10^6$ km^2, for the Canada/Alaska area, and of $(20.75+/-0.32)\cdot10^6$ km^2 over Northern Eurasia. We compare the seasonal variation with two existing satellite datasets: one from the NSIDC (National Snow and Ice Data Center, Boulder, USA) derived from optical sensors, and one from IMS (Interactive Multisensor Snow and Ice Mapping System) derived from different sensors, available since 1997. Differences occur over high mountains as topographic effects hamper our method to clearly distinguish the snow signal. In some other areas we are more confident about our method. Also short snow-free episodes during winter cannot be detected, but our interest is to clearly define a long snow- / ice-free period characterizing the summer. Good concordances during key climatic months (March-April-November-December) are found between the series which allow us to study climate variability in further work.

Keywords: Passive microwave brightness temperature, SSM/I remote sensing data, snowcover extent, northern high latitudes.

INTRODUCTION

Snow cover is a key climatic parameter characterized by high albedo and a positive feedback on temperature changes (1): the less snow, the more solar energy is absorbed, resulting in an increase in temperature and thus a decrease in snow coverage. Snow Cover Extent (SCE) is important in the Northern Hemisphere, as it can reach ~50% (about $47\cdot10^6$ km^2) of the land during winter (2). The important impact of snow cover variation on the climate (3) implies accurate snow cover maps in order to improve global circulation model simulations (4), and therefore to better understand interactions between climate and cryosphere.

Snow cover extent is also well recognized as a climate indicator (5,6). Survey of its variability over several years provides information on the global warming effect at both regional and global scales. Increase in surface temperature, El Nino/La Nina cycles or the North Atlantic Oscillation have an impact on SCE (1) leading to a decline in the snow cover area by 10% since 1972 (7). This melting could affect the surface hydrological cycle noticeably.

Studying SCE is of major interest even more over high latitudes where a significant increase in temperature is expected. Unfortunately, ground based meteorological station networks appear insufficient for a global study over the high latitudes (>50°N). For a few decades, satellite data has

been an alternative source, providing a vast amount of information concerning the earth system. Independent of clouds and solar radiation (compared to optical sensors), microwave radiometers measure the energy emitted by the surface. At 19 GHz and 37 GHz, the atmosphere has a small contribution. Several methods have been validated to map SCE (8,9) from passive microwaves. We are presenting a simple method based on SSM/I (Special Sensor Microwave Imager) sensor data, available since August 1987. After a brief description of the microwave dataset and method, seasonal SCE is presented and compared to other databases.

METHODS

The method to derive daily snow maps is based on microwave brightness temperatures from SSM/I (Special Sensor Microwave Imager). This study is carried out within the framework of a wider research on surface parameters such as surface temperature and fraction of water surface (10). A limit of their method is the presence of snow and/or frozen water on the ground. Our first objective is to detect and avoid snow-covered areas that could bias the derived parameters. Thus, we define a snow-covered period, characterized by beginning/end dates (first/last day with snow on the ground) and its length (number of days). These features might be of interest for climate variability studies (3).

The database

This work is based on vertically polarized brightness temperatures acquired by the SSM/I sensors at 19 and 37 GHz. The data are distributed (11) by the NSIDC (National Snow and Ice Data Center, Boulder, Co, USA). They are dependent on two variables characterizing the surface coverage: emissivity (= capacity to emit energy) and temperature. In this part of the electromagnetic spectrum, atmosphere contribution is quite low.

Data are presented in an equal area grid, the EASE-Grid (Equal Area Scalable Earth), with a spatial resolution of 25 km×25 km. Because of this rather low resolution (each pixel covering a 625 km^2 area), local applications are inadequate. However, for global study purposes, it has the advantage of covering the entire surface in a few days. Indeed, the repeat orbit provides at least one measurement every other day for SMMR and twice a day in the best case for SSM/I.

Ground snow depths are provided by Environment Canada available from their website http://www.climate.weatheroffice.ec.gc.ca/prods_servs/cdcd_iso_f.html.

Area of interest

The purpose of this study is to create a SCE database which covers the Northern High Latitudes (latitudes >50°N) where permafrost is found: the northern part of the North American continent (Canada and Alaska) and the northern part of Eurasia (Figure 1).

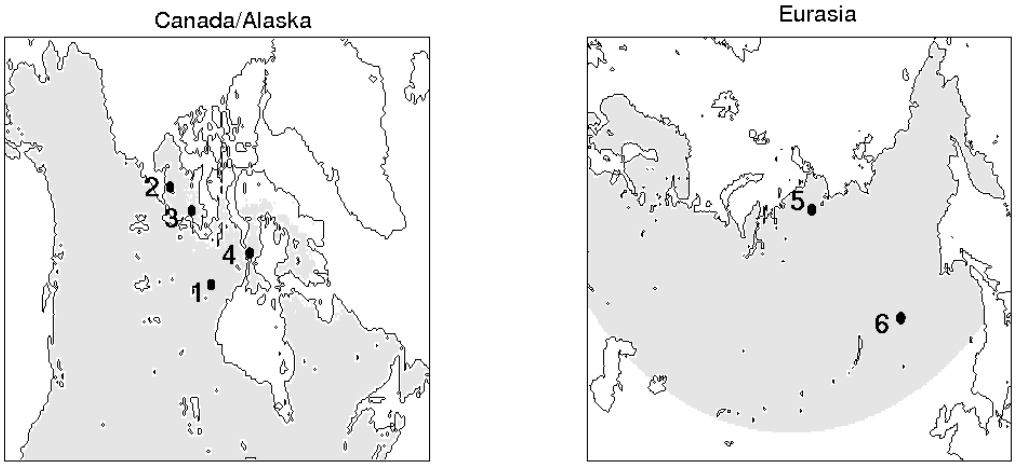

Figure 1: Areas of interest in grey (Canada/Alaska on the left, Eurasia on the right); 1: Baker Lake meteorological station (64°18N, 96°5W); 2: Holman (70°46N, 117°48W); 3: Cambridge Bay (69°6N, 105°8 W); 4: Repulse Bay (66°31N, 86°13W).

Note that we excluded areas of permanent snow/ice (Greenland and most islands in the Arctic Ocean), based on land cover classification (12). Open water areas larger than one pixel are also masked as well as coastal pixels, because the sensor footprint is larger than the EASE Grid resolution. This induces a contamination of these pixels by the nearby open water (oceans/sea). In the microwave spectrum, open water has a typical low emissivity compared to any other surface (13), decreasing significantly the brightness temperature.

Processing

We defined an index d*T*, as:

$$\mathrm{d}T = \frac{(Tb37V - Tb19V)}{Tb19V} \quad , \tag{1}$$

Tb19V and *Tb37V* referring to vertically polarized brightness temperatures at 19 and 37 GHz. d*T* has a seasonal variation (Figure 2), and Grody and Basist (14) found that (Tb37V-Tb19V) inferior to a threshold is a signature of the presence of snow. The idea of using a difference in brightness temperature is based on the different behaviours observed for these channels (8). As snow is a scattering media (14), it leads to a decrease in emissivity, thus a decrease in the brightness temperature. As this effect is more important at high frequencies (8,14), more important at 37 GHz than at 19 GHz, d*T* decreases when snow is present on the ground. Several studies use this spectral signature to discriminate snow (9,15). Grody and Basist (9) recommend the use of the 85 GHz channel for shallow snow layers. We chose to focus only on two channels, because they are common to the SMMR and SSM/I sensors. For climate variability discussions, longer time series are needed.

Figure 2 is an example of daily d*T* during one year (2000) for a pixel relative to the Baker Lake meteorological station (1 on Figure 1). The seasonal variation is noticeable and it is possible to distinguish snow-covered and snow-free seasons. As d*T* is subject to fluctuations, especially during spring (and to a lesser extent during fall) when freezing/thawing cycles occur (grey line in Figure 2, days of the year: 130-150), a 23-day window median filter is applied on d*T* (bold line in Figure 2). Wet snow is a good emitter in the microwave region (16) at both 19 and 37 GHz leading to a small difference between Tb(19 GHz) and Tb(37GHz). This results in d*T* higher for wet snow than for dry snow. Moreover, satellite overpasses provide measurements in the morning (around 06h00 am local time) and the afternoon (around 06h00 pm local time). Considering the remark above, associated with the fact that melting snow events happen more often during the afternoon, only morning data are kept (17).

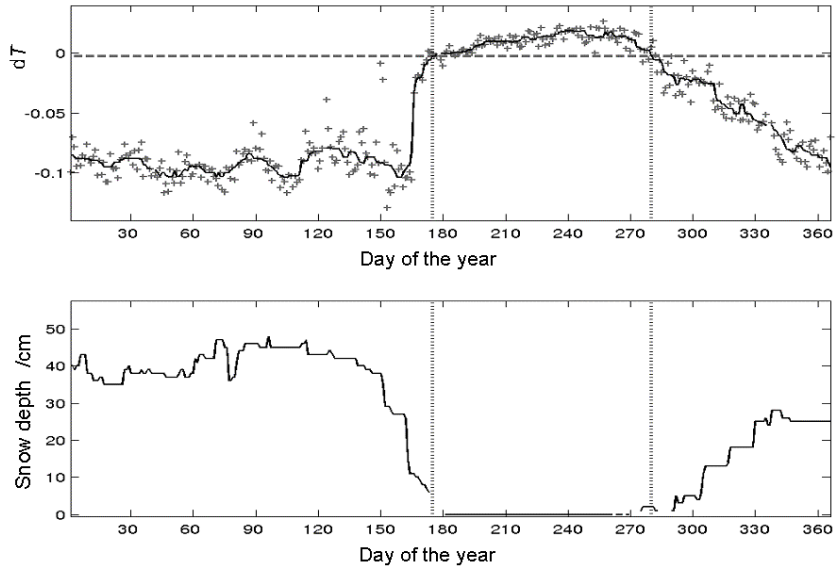

*Figure 2: Above: d*T *variation (+), filtered d*T *(black line), threshold (dashed horizontal line), day of beginning / end of snow free period (vertical dotted lines) for the year 2000, for the pixel relative to the Baker Lake station (1 on Figure 1); Below: Snow depth measurements at the station.*

As shown in Figure 2, a threshold (horizontal dashed line) is used to define days corresponding to the beginning and the end of the snow-free season (when the smoothed series - black line – crosses the threshold). The threshold cannot be a constant value as the amplitude and dT are dependent on the surface (bare soil, dense forested taiga), but also on the satellite local time overpass. Moreover, the 25-year series is derived from two different sensors (SMMR and SSMI), on board several satellites (Nimbus 7, DMPS-F8, DMSP-F11, DMSP-F13). Problems of intercalibration may imply a bias between the different series (17). Grody and Basist (9) applied a constant threshold but needed other criteria on brightness temperatures. A different approach is proposed with an adaptative threshold. From the non-filtered dT values, a mean value and a standard deviation can be computed for the summer period. We chose the period between day 183 (2 July) and 243 (31 August), as the NSIDC snow cover dataset shows no snow cover for the entire area of study.

From dT time series, we derive for each pixel and each year, a summer mean $\langle \mathrm{d}T \rangle_{summer}$ associated with the standard deviation σ. The threshold *th* is then defined as:

$$th = \langle \mathrm{d}T \rangle_{summer} - 2\sigma \qquad (2)$$

The beginning and end (vertical dotted line in Figure 2) of a snow- /ice-free period are deduced from the threshold and the filtered ratio.

This approach using a median filter may appear very selective (especially for the beginning of the snow-free period) but, as mentioned above, our objective was to carefully avoid snow-/ice-covered surfaces (10). But, for large-scale application, the data presented below show interesting results in good accordance with existing datasets.

RESULTS

Seasonal Snow Cover Extent

Figure 3 presents the mean Snow Cover Extent (SCE) over the 1987-2001 period for the Northern High Latitudes (between 50°N and 75°N) derived from the method described above (black line with dots).

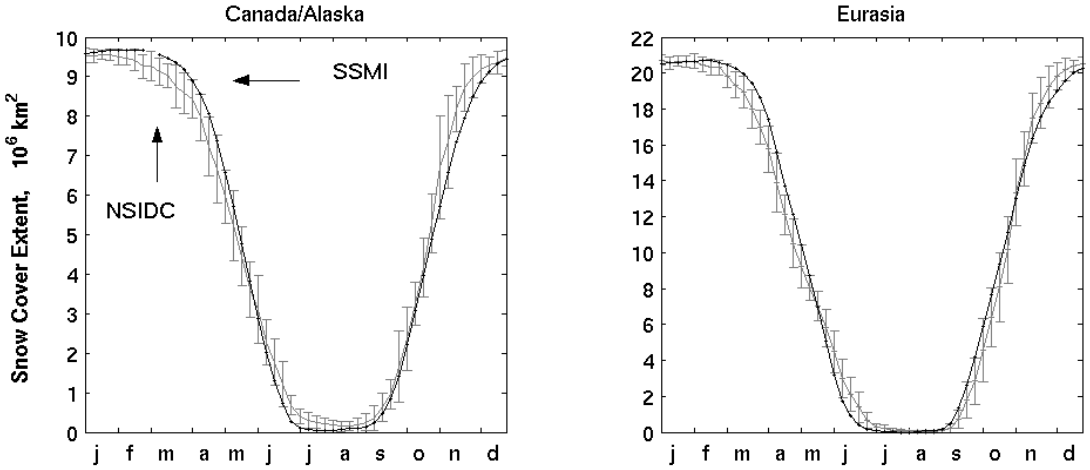

Figure 3: Seasonal variation of weekly SCE derived from SSM/I (this work, black line) and from AVHRR (NSIDC, grey line with error bars) for the 1988-2001 period. Error bars correspond to one standard deviation.

A maximum SCE of (9.69 +/- 0.06)·10^6 km^2 is found during mid-February for Canada/Alaska, and of (20.75 +/- 0.32)·10^6 km^2 for Eurasia. In this figure, a weekly computed SCE series is compared to the NSIDC Northern Hemisphere EASE-Grid Weekly Snow Cover and Sea Ice Extent (grey line with error bars) Version 2 product derived from the AVHRR (Advanced Very High Resolution Radiometer) on board the NOAA satellites (18). The comparison shows good agreement, with an overestimation (underestimation) for spring (fall) periods with a maximum of +(-) 6%. Amstrong and

Brodzik (2) compared microwave and visible products, and found differences mostly located in the southern limit of the SCE (we focused on higher latitudes, i.e. >50°N, to reduce this effect). Both series have their strengths and weaknesses, microwaves showing limits in detecting wet snow (19) and shallow snow layers (<5 cm) (16,20), whereas visible measurements are hampered by clouds (2). Only the last cloud-free view of the week is used to derive the weekly SCE, which can be a limit during the spring period as rapid changes can occur in a week through melting/thawing events.

Our daily approach is also compared (Figure 4) to another daily satellite snow cover database from the IMS (Interactive Multisensor Snow and Ice Mapping System,[21]) using several sensors (POES, GOES, MODIS, GMS). Available since 1997 for the entire northern hemisphere, we used the 24 km x 24 km resolution series as it is close to the EASE-Grid. Romanov et al. ([25]) pointed out the importance of adding the SSM/I information to enhance the accuracy of their analysis. Figure 4 shows the mean daily seasonal variation of SCE over the 1997-2001 period for Canada/Alaska (left) and Northern Eurasia (right).

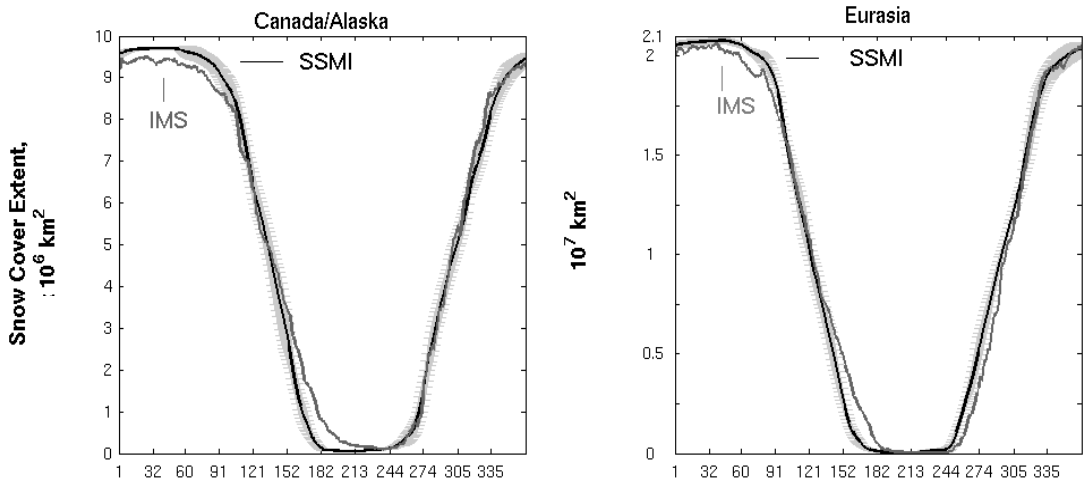

Figure 4: Seasonal variation of daily SCE (for the 1997-2001 period) derived from SSM/I (this work, black line with error bars) and IMS product (grey line) for the 1988-2001 period. Error bar corresponds to one standard deviation; Left Figure stands for Canada/Alaska, and right Figure for Northern Eurasia.

The maximum winter coverage for both areas occurs during February. Table 1 summarizes the mean maximum values of the different series over Canada/Alaska and Eurasia areas. Two SSM/I maximums are presented corresponding to the different time periods covered by the NSIDC and IMS databases. For both Canada/Alaska and Eurasia, the SSM/I algorithm well reproduces the maximum snow extent compared to the other satellite datasets.

Table 1: Mean maximum SCE derived from SSMI approach (1988-2001), IMS product (1997-2001), and NSIDC SCE (1988-2001), ·10^6 km^2.

	SSMI (mean 1997-2001)	**IMS** (mean 1997-2001)	**SSMI** (mean 1988-2002)	**NSIDC** (mean 1988-2000)
Canada/Alaska	9.75+/-0.02	9.67+/-0.05	9.68+/-0.06	9.56+/-0.14
Eurasia	20.90+/-0.13	20.87+/-0.18	20.69+/-0.38	20.73+/-0.27

A similar pattern is found from the two approaches despite some discrepancies (Figure 4) during winter and late spring/beginning of summer (days 150-180, i.e. mid-June to July). During fall, the trend over Canada/Alaska is well reproduced, even if the use of a median filter does not allow rapid variations to be related (around days 305 and 335 on the left Figure 4). A noticeable difference exists during fall over Northern Eurasia around days 160-190.

Winter discrepancy

During winter, for both regions a greater SCE is found with our method than with IMS. Analyses of maps (Figure 5 and 6 related to day 36 for Canada/Alaska and day 72 for Eurasia) show differences over the 5-year comparison. A value of 1 corresponds to 1 of 5 years covered with snow. Over Canada/Alaska (Figure 5), the IMS product shows less snow over the western part of the Prairies, next to the Rocky Mountains.

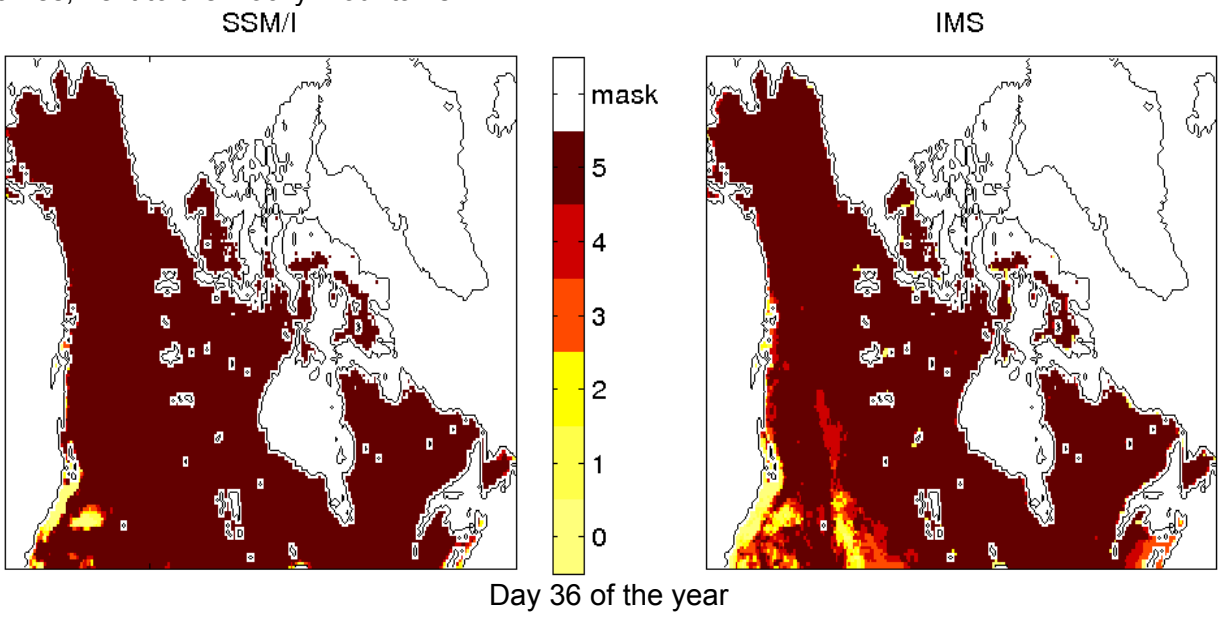

Figure 5: Frequency of presence of snow (from 0 to 5 years) for the 1997- 2001 period, derived from SSM/I (left) and IMS (right), for day 36 of the year over Canada/Alaska.

Analysis of the d*T* variation for pixels of disagreements shows strong fluctuations during the winter period. However, these d*T* are quite different from the summer (=snow-free) period and confidence can be given to microwave-derived SCE. Nevertheless, short snow-free periods during winter are not detected with our approach.

Over Eurasia (Figure 6), differences appear over the Himalayas (high mountains), near the South-East border of our area (50°N latitude). But topographic effects do not allow the snow signal to be distinguished clearly (same remark over the Rocky Mountains in Canada /Alaska, day 175).

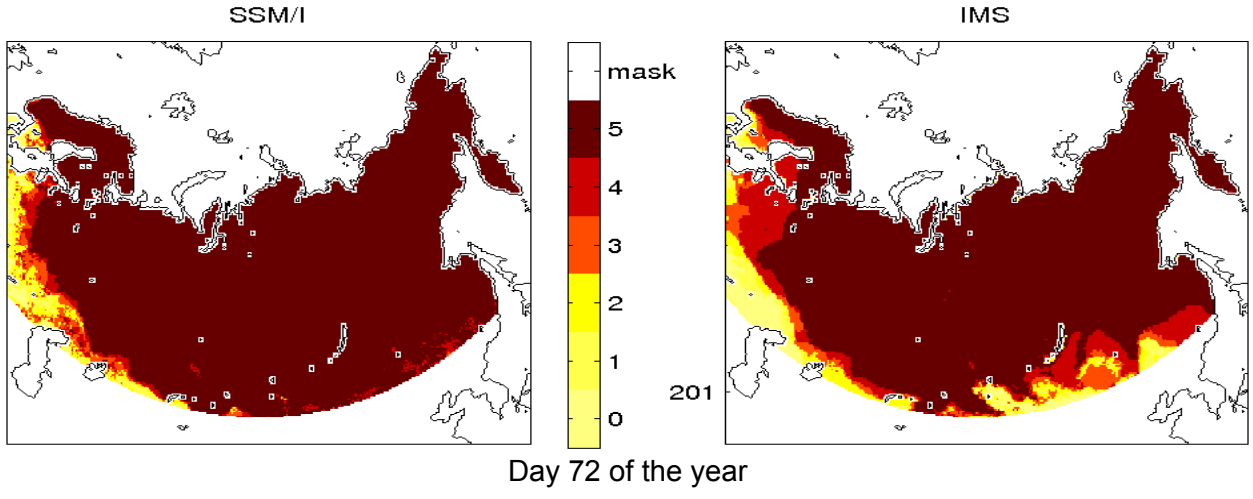

Figure 6: Frequency of presence of snow (from 0 to 5 years) for the 1997- 2001 period, derived from SSM/I (left) and IMS (right), for day 72 of the year over Eurasia.

Spring-summer discrepancy

The beginning of summer is characterized by marked differences between the two approaches with IMS giving a larger SCE (Figure 7 for day 168 over Eurasia and Figure 8 for day 175 over Canada/Alaska) (middle). Figure 7 presents an example of d*T* (during the year 1998) values for a pixel (where large differences occur between the datasets, position 5 on Figure 1) located north-east of the Ob basin (Eurasia).

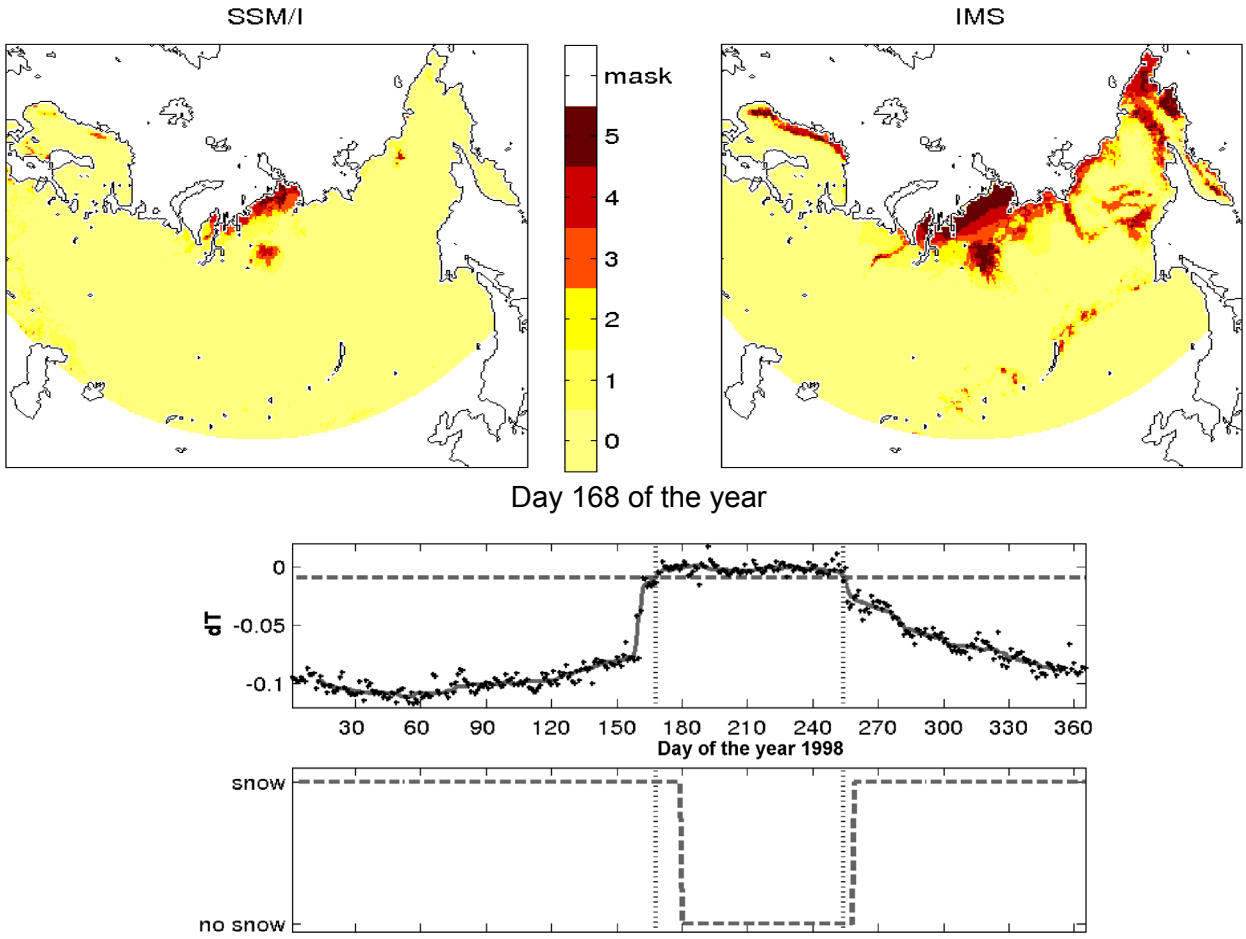

*Figure 7, above: Frequency of presence of snow (from 0 to 5 years) over the 1997-2001 period, derived from SSM/I (left) and IMS (right), for day 168 over Eurasia; Middle: d*T *values with beginning and end of snow-free period for one pixel (position 5 on Figure 1), year 1998 ; Below: snow-free seasons from SSM/I (vertical dotted lines) and IMS snow information (dashed line).*

If we focus around day 168, our method detects snow earlier than IMS during the five years. IMS found snow until days around 180 (dashed grey line) characterized by a stable d*T* (middle in Figure 6), obviously higher than winter values. The five years present the same patterns.

Over Canada/Alaska (Figure 8), a noticeable difference is found over the Rocky Mountains in the western part of the area. High mountains are characterized by winter and summer d*T* values that are pretty similar, suggesting a topographic effect (same pattern over the Himalayas). This is a limit of our approach and further work should be performed to mask high-elevated areas. Another important area of discrepancies is located over Victoria Island and north of the Nunavut Territories (North West of Hudson Bay, Figure 8). IMS is still detecting snow while SSM/I is not.

Three meteorological stations providing snow depth are used to validate our results: two are located on Victoria Island (Cambridge Bay, position 3 on Figure 1 and Holman, position 2 on Figure 1) and one northwest of Hudson Bay (Repulse Bay, position 4 on Figure 1). Figure 9 shows examples for the year 2000. For each station, d*T* is presented with the threshold and days of beginning/end of the snow-free period. Figures 9b, d and f report snow depth at the station, presence of snow from IMS and from SSM/I d*T*.

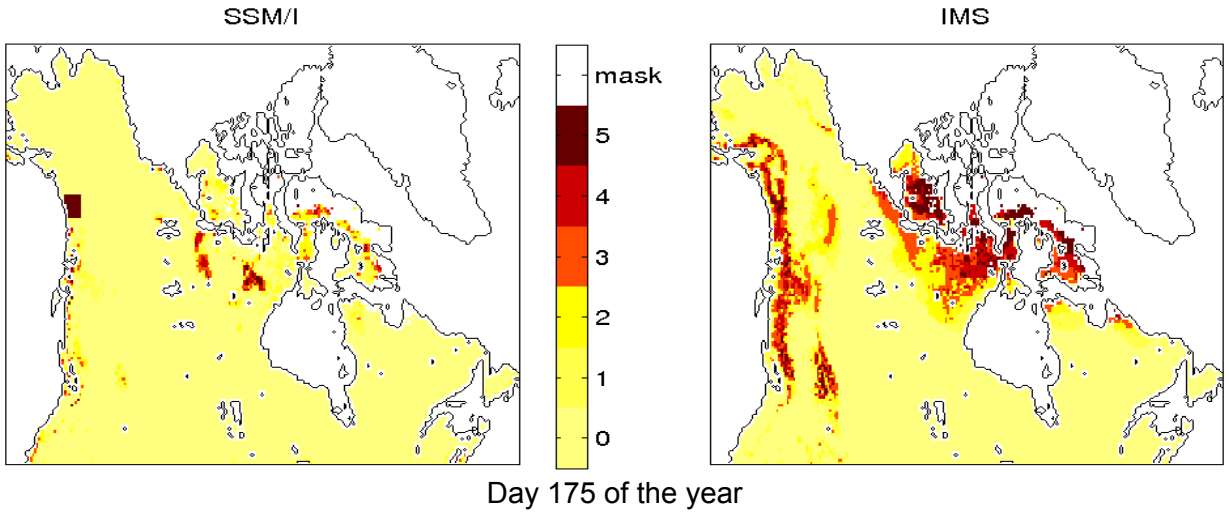

Figure 8: Frequency of presence of snow (from 0 to 5 years) for the 1997- 2001 period, derived from SSM/I (left) and IMS (right), for day 175 over Canada/Alaska

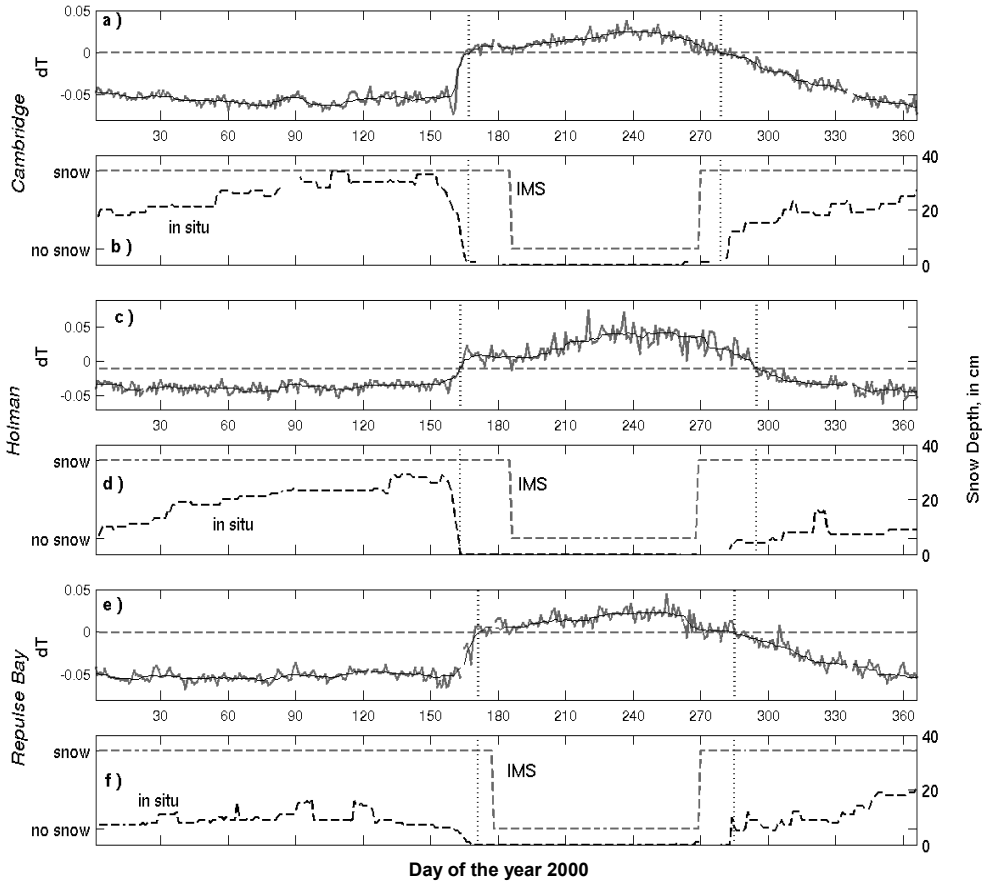

Figure 9: dT values (a,c,e) with beginning and end of snow-free period for pixels relative to three meteorological stations for the year 2000 : a,b) for Cambridge Bay (position 3 on Figure 1), c,d) for Holman (position 2 on Figure 1), e,f) for Repulse Bay (position 4 on Figure 1) ; b,d,f present in situ *snow depth in cm (black dashed line) with right axis, and IMS snow detection (grey dashed line).*

Definition of a day characterizing the complete melting of snow is difficult. The three examples shown in Figure 9 for the year 2000 suggest that IMS (dashed line) consistently found more snow than SSM/I (same observations for the other years). *In situ* measurements (dash-dotted lines) revealed a closer agreement with our results for that region. The increase in d*T* during the beginning of summer (around day 170) associated with low vegetation (Tundra (12)) is indicative of a clear change occurring at the surface (disappearance of snow). These observations are confirmed by

Wang et al. (22) who found that NOAA snow charts overestimate SCE over Arctic regions during June.

Fall discrepancies over Eurasia

During fall (Figure 10, day 284), IMS reports less snow over an area located in the eastern part of Eurasia where a constant snow cover over the 5-year period is found by SSM/I. An example of d*T* for a pixel (position 6 on Figure 1) of this area shows (Figure 10, middle) a slow decrease during fall that should be relative to the slow increase in snow depth. As shallow snow layers (<4-5 cm, 18,23) are transparent to microwaves at low frequencies (9,14), it is difficult to clearly identify with our method a day related to the end of the snow-free season.

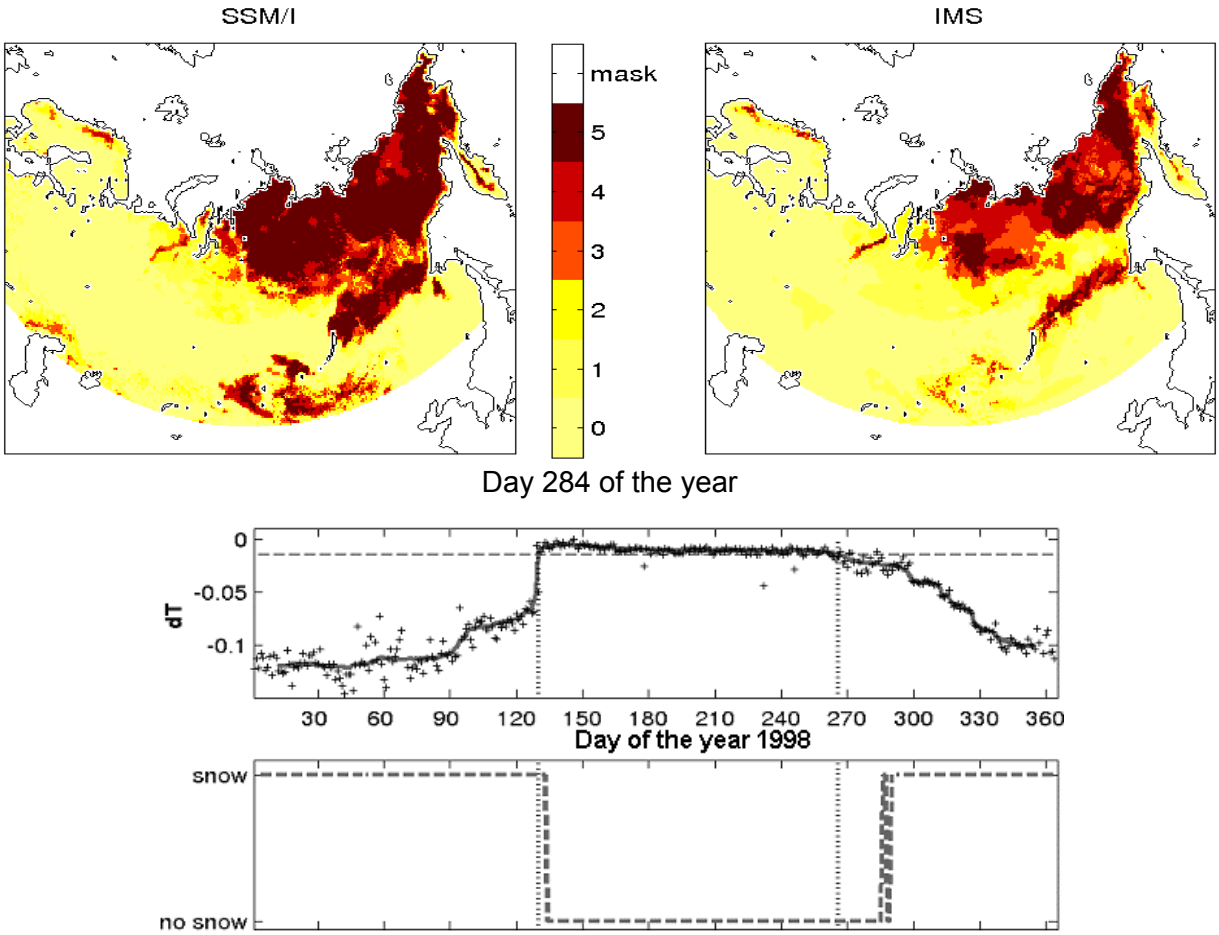

*Figure 10: Above: Frequency of presence of snow (from 0 to 5 years) over the 1997-2001 period, derived from SSM/I (left) and IMS (right), for day 284 over Eurasia; Middle: d*T *values with beginning and end of snow-free period for one pixel (position 6 on Figure 1), year 1998 ; Below: snow-free seasons from SSM/I (vertical dotted lines) and IMS snow information (dashed line).*

Despite the discrepancies due to different characteristics of the datasets used by the three approaches, our results correctly reproduce the SCE during several months (Figure 4): March-April-May and October-November-December. This is an interesting result, as (6), CLIC report (5) noticed a significant impact of climate variability occurring during these periods (7). Thus interannual variability will be explored in further work.

CONCLUSIONS

Passive microwaves present interesting characteristics for the study of SCE over Northern High Latitudes. Slightly influenced by the atmosphere over the continent, they allow surface parameters (as surface temperature (10) and open water extent (24) to be derived. Here, we present a simple method to detect the start / end of a snow free period by means of passive microwaves. To minimize intersensor bias (calibration and slightly different measurement time (25,26)), a method

based on an adaptative threshold was developed. Results are compared with two datasets: one derived from AVHRR sensors from 1966 to 2000 on a weekly basis, and the other one blending data from several sensors (IMS (23)), available since 1997. Some discrepancies appear between the different approaches. Our method showed a limitation in correctly detecting snow signals over mountains. Short snow-free periods during winter and shallow layers (<5 cm) during fall are not detected. But elsewhere, even if regarded cautiously, comparisons with *in situ* measurements over most permafrost areas (regions of major interest to our studies) seem to confirm the validity of our SCE results.

Moreover, very similar results for the different series are found during key months (November/December and March/April (6,7)) for climate studies. This simple method could easily be applicable to SMMR (Sensor Multichannel Microwave Radiometer) data, available between 1978 and 1987. Combining the two datasets is of interest for climate purposes, as the time series could be extended to more than 25 years.

ACKNOWLEDGEMENTS

Research funding was provided by the Canadian Fund for Climate and Atmospheric Sciences, the Natural Sciences and Engineering Research Council of Canada, Environment Canada (CRYSYS project), the French Ministère de la Recherche (ACI observation de la terre, ACI changement climatique) and the Ministère des Affaires Étrangères (Coopération France-Québec).

REFERENCES

1 Groisman P Y, T R Karl & R W Knight, 1994. Observed impact of snow cover on the heat balance, and the rise of continental spring temperatures. Science, 263: 198-200

2 Armstrong R L & M J Brodzik, 2001. Recent Northern Hemisphere Snow Extent: a comparison of data derived from visible and microwave satellite sensors. Geophysical Research Letters, 28(19): 3673-3676

3 ACIA, 2004. Impacts of a warming Arctic: Arctic Climate Impact Assessment (Cambridge University Press) http://www.acia.uaf.edu/

4 Ramsay B H, 1998. The interactive multisensor snow and ice mapping system. Hydrological Processes, 12: 1537-1546

5 CLIC, 2001. CLImate and Cryosphere project. In: I Allison, R G Barry & B Goodison, Science and co-ordination plan, WRCP-114, WMO/ TD 1053

6 Brown R D, 2000. Northern Hemisphere snow cover variability and change, 1915-1997. Journal of Climate, 13: 2339-2355

7 Serreze M C, J R Walsh, F S Chapin III, T Osterkamp, M Dyurgerov, V Romanovsky, W D Oechel, J Morison, T Zhang, & G Barry, 2000. Observational Evidence of Recent Change in the Northern High-Latitude Environment. Climatic Change, 46: 159-207

8 Mätzler C, 1994. Passive microwave signatures of landscapes in winter. Meteorol. Atmos. Phys., 54 : 241-260.

9 Grody N C & A N, A N Basist, 1996. Global identification of snowcover using SSM/I measurements. IEEE Transctions of Geoscience and Remote Sensing, 34: 237-249

10 Fily M, A Royer, K Goïta & C Prigent, 2003. A simple retrieval method for land surface temperature and fraction of water surface determination from satellite microwave brightness temperatures in sub-arctic areas. Remote Sensing of Environment, 85: 328-338

11 Armstrong R L, K W Knowles, M J Brodzik & M A Hardman, 2003. DMSP SSM/I Pathfinder daily EASE-Grid brightness temperatures. National Snow and Ice Data Center (Boulder, CO, USA) http://nsidc.org/data/nsidc-0032.html. Also available on CD-ROM

12 Cihlar J & J Beaubien, 1998. Land Cover of Canada Version 1.1. In Special Publication NBIOME Project, Canada Center for Remote Sensing and the Canadian Forest Service (Ottawa, Ontario), Natural Resources Canada. Available on CD-ROM from the Canada Center for Remote Sensing

13 Prigent C, W B Rossow, & E Matthews, 1997. Microwave land surface emissivities estimated from SSM/I observations. Journal of Geophysical Research, 102(D18): 21867-21890

14 Grody N C & A N Basist, 1997. Interpretation of SSM/I measurements over Greenland. IEEE Transactions of Geoscience and Remote Sensing, 35(2): 360-366

15 Chang A T C, J L Foster & D K Hall, 1987. Nimbus-7 SMMR derived global snow cover parameters. Annals of Glaciology, 9: 39-44

16 Armstrong R L & M J Brodzik, 2002. Hemispheric-scale comparison and evaluation of passive-microwave snow algorithms. Annals of Glaciology, 34: 38-44

17 Derksen C, E LeDrew, A Walker & B Goodison, 2000. Influence of sensor overpass time on passive microwave-derived snow cover parameters. Remote Sensing of Environment, 71: 297-308

18 Armstrong R L & M J Brodzik, 2002. Northern Hemisphere EASE-Grid Weekly Snow Cover and Sea Ice Extent Version 2. National Snow and Ice Data Center (Boulder, CO, USA) Available on CD-ROM

19 Walker A E & B E Goodison, 1993. Discrimination of a wet snow cover using passive microwave satellite data. Annals of Glaciology, 17: 307-311

20 Derksen C & E LeDrew, 2000. Temporal and spatial variability of North American prairie snow cover (1988-1995) inferred from passive microwave-derived snow water equivalent imagery. Water Resources Research, 36(1): 255-266

21 NOAA / NESDIS / OSDPD / SSD, 2004. IMS Daily Northern Hemisphere Snow and Ice Analysis at 4 km and 24 km Resolution, Boulder, CO: National Snow and Ice Data Center. Digital media.

22 Wang L, M Sharp, R Brown, C Derksen & B Rivard, 2005. Evaluation of spring snow covered area depletion in the Canadian Arctic from NOAA snow charts. Remote Sensing of Environment, 95: 453-463

23 Romanov P, G Gutman & I Csiszar, 2000. Automated Monitoring of Snow Cover over North America with Multispectral Satellite Data. Journal of Applied Meteorology, 39: 1866-1880

24 Mialon A, A Royer & M Fily, 2005. Wetlands seasonal dynamics and interannual variability over Northern high latitudes, derived from microwave satellite data. Journal of Geophysical Research, 110, D17102, doi:10.1029/2004JD005697

25 Abdalati W, K Steffen, C Otto & K C Jesek, 1995. Comparison of brightness temperatures from SSM/I instruments on the DMSP F8 and F11 satellites for Antarctica and the Greenland ice sheet. International Journal of Remote Sensing, 16(7): 1223-1229

26 Stroeve J, J Maslanik & L Xiaoming, 1998. An Intercomparison of DMSP F11 and F13 derived Sea Ice Products. Remote Sensing of Environment, 64(2): 132-152